



Original Articles

Exosomal lncCRLA is predictive for the evolvement and development of lung adenocarcinoma



Shuai Lin ^{a,1}, Chenyang He ^{a,1}, Lingqin Song ^a, Liangzhang Sun ^b, Renyang Zhao ^a, Weili Min ^a, Yang Zhao ^{a,*}

^a Department of Oncology, The Second Affiliated Hospital of Xi'an Jiaotong University, Xi'an, Shaanxi Province, 710004, PR China

^b Thoracic Department, The Second Affiliated Hospital of Xi'an Jiaotong University, Xi'an, Shaanxi Province, 710004, PR China

ARTICLE INFO

Keywords:
lncCRLA
Lung adenocarcinoma
Biomarker
Tumor evolvement

ABSTRACT

Lung adenocarcinoma, the most common histological subtype of non-small cell lung cancer, exhibits heterogeneity that enables adaptability, limits therapeutic success, and remains incompletely understood. Our team uncovers that lncRNA related to chemotherapy resistance in lung adenocarcinoma (lncCRLA) is preferentially expressed in lung adenocarcinoma cells with the mesenchymal phenotype. lncCRLA can not enhance chemotherapy resistance in lung adenocarcinoma due to its binding to RIPK1 in exosomes, which is released into intercellular media and transferred by exosomes from mesenchymal-like to epithelial-like cells. However, plasmatic lncCRLA corresponding to tissue lncCRLA functions as a preferred biomarker to reflect the response to chemotherapy and disease progression of lung adenocarcinoma. Through single-cell sequencing, RNA-Mutect technique and spatial transcriptomics, a handful of hybrid EMT cells with elevated lncCRLA are characterized as the origin of lung adenocarcinoma, which are indiscriminated from hybrid EMT cells by the in-depth sequencing. Plasmatic lncCRLA is properly predictive for the preinvasive lesion of lung adenocarcinoma that would evolve to invasive lesion. That notion is confirmed by a brand-new transgenic mouse model in which EMT is tracked by Cre and Dre system. Dasatinib is potential to hinder the spontaneous progression from preinvasive to invasive lesion of lung adenocarcinoma. Together, plasmatic lncCRLA is defined as a brand-new circulating biomarker to predict the occurrence and evolvement of lung adenocarcinoma, a light for early detection of lung adenocarcinoma.

Accession number (GEO)

GSE235782.

1. Introduction

Lung cancer accounts for the highest cancer incidence and mortality worldwide and in China with 5-year survival rate of less than 20% [1–3]. Lung adenocarcinoma was the most common histological subtype of non-small cell lung cancer (NSCLC) with sharp increase in the incidence [1,4]. Despite several big progresses, there are still a large percent of lung adenocarcinoma patients without the available therapeutic options due to tumor metastasis and acquired resistance to therapy [5–7].

Epithelial-mesenchymal transition (EMT) was depicted as a tumor

biological process to induce tumor metastasis and resistance to therapy [8,9]. This notion was supported by our observation that phosphorylated Caspase-8 at tyrosine 380 (*p*-Casp8) by activated c-Src was able to trigger EMT-related metastasis and yield the resistance to paclitaxel in lung adenocarcinoma [10,11]. In addition, we observed that a brand-new long non-coding RNA (lncRNA), lncCRLA, was expressed during EMT process of lung adenocarcinoma [10,11]. Recently, the evidence was mounting to uncover that intermediate or hybrid EMT took major part to reflect tumor heterogeneity and development [9,12,13]. Moreover, circulating tumor DNAs and lncRNAs were potential to modify the tumor diagnosis and therapy [14,15]. Now, it is urgent to elucidate the underlying mechanism to discover the role of lncCRLA on EMT process and development of lung adenocarcinoma.

In this study, lncCRLA was associated with mesenchymal or hybrid EMT phenotype in lung adenocarcinoma, that was transferred from

* Corresponding author.

E-mail addresses: voyage420@163.com (S. Lin), xiaoguanghcy@163.com (C. He), songlingqin@163.com (L. Song), sunliangzhang@126.com (L. Sun), zhaoxy2023@126.com, happy2018@stu.xjtu.edu.cn (R. Zhao), mwl791218@126.com (W. Min), szhaoy@126.com, szhaoy@xjtu.edu.cn (Y. Zhao).

¹ Equal contribution.

<https://doi.org/10.1016/j.canlet.2023.216588>

Received 25 August 2023; Received in revised form 7 November 2023; Accepted 4 December 2023

Available online 12 December 2023

0304-3835/© 2023 The Authors. Published by Elsevier B.V. This is an open access article under the CC BY-NC-ND license (<http://creativecommons.org/licenses/by-nd/4.0/>).

Abbreviation	
lncCRLA	lncRNA related to chemotherapy resistance in lung adenocarcinoma
NSCLC	non-small cell lung cancer
lncRNA	long non-coding RNA
p-Casp8	phosphorylated Caspase-8 at tyrosine 380
CM	culture medium
FITC	fluorescein isothiocyanate
Vim	vimentin
E-cad	E-cadherin
CR	complete response
PR	partial response
SD	stable disease
PD	progressive disease
scRNA-seq	single-cell RNA sequencing
t-SNE	t-stochastic neighbor embedding
CNVs	copy number variations
ST	spatial transcriptomics
CT	computed tomography
STR	short tandem repeat
CRISPR	Clustered regularly interspaced short palindromic repeats
AJCC	American Joint Committee on Cancer
CR	complete remission
PR	partial remission
SD	stable disease
PD	progressive disease
RECIST	response evaluation criteria in solid tumors
LNA-ISH	LNA based in situ hybridization
EDTA	ethylenediaminetetraacetic acid
IHC	immunohistochemistry
MET	mesenchymal–epithelial transition
scRNA-seq	single-cell RNA sequencing
NCI	National Cancer Institute
STR	short tandem repeat

mesenchymal-like to epithelial-like cells. Plasmatic lncCRLA level representing tissue lncCRLA level was characterized as a predictor for the response to chemotherapy in lung adenocarcinoma. Through single-cell sequencing and spatial transcriptomics, a bunch of hybrid EMT cells with elevated lncCRLA were depicted to be the origin of lung adenocarcinoma. Plasmatic lncCRLA was properly predictive for the pre-invasive lesion of lung adenocarcinoma that would evolve to invasive lesion. That notion was confirmed by transgenic mouse model in which EMT was tracked by Cre and Dre system.

2. Materials and methods (Supplementary data)

2.1. Results

2.1.1. lncCRLA is highly expressed in the mesenchymal-like lung adenocarcinoma cells

We previously reported that phosphorylated Caspase-8 at tyrosine 380 by activated c-Src was the crux to trigger EMT in lung adenocarcinoma [10,11]. According to p-Casp8 expression, lung adenocarcinoma cells were classified into the mesenchymal-like (*p*-Casp8-positive: A549+control and H522+Casp8) and the epithelial-like (*p*-Casp8-negative: A549+Src/Casp8 shRNA and H522+control) phenotype [10, 11]. *p*-Casp8-expressing A549+control and H522+Casp8 cells presented the mesenchymal-like characteristics (E-cad⁺Vim⁺, Fig. S1A). The epithelial-like A549 cells with c-Src shRNA in which Caspase-8 phosphorylation was impaired were sensitive to paclitaxel with a significant increase in apoptosis (Fig. 1A and B). Mesenchymal-like A549+control and H522+Casp8 cells in which Caspase-8 function was blocked by its phosphorylation were resistant to paclitaxel with approximately 10% of necroptosis (Fig. 1A), while the epithelial-like A549+Casp8 shRNA and H522+control cells in which Caspase-8 was deficient presented 25–30% of necroptosis to paclitaxel (Fig. 1B). This observation was elucidated by our previous report that lncCRLA reduced necroptosis in lung adenocarcinoma with *p*-Casp8-induced EMT due to its binding RIPK1 [10].

lncCRLA was upregulated by the Wnt-related promoter in the process of EMT [10]. The northern blot exhibited the higher level of lncCRLA in the mesenchymal-like A549 and H522 cells compared with the epithelial-like cells (Fig. S1B), that was supported by immunofluorescent analysis (Fig. 1C). We next investigated the underlying mechanism for lncCRLA upregulation in lung adenocarcinoma. No genomic amplification of lncCRLA was detected in the mesenchymal-like A549 and H522 cells (Fig. S1C). Inhibition of DNA methyltransferase exerted no influence on lncCRLA expression in the mesenchymal-like lung adenocarcinoma cells (Fig. S1D). Furthermore, there was a smaller number of

lncCRLA in the nuclei as compared with that in cytoplasm (Figs. S1E and S1F). Together, lncCRLA was upregulated through *p*-Casp8-induced EMT in the mesenchymal-like lung adenocarcinoma.

2.1.2. Exosomal lncCRLA from mesenchymal-like lung adenocarcinoma cells is secreted and intercellularly transferred

To examine whether lncCRLA was present in extracellular milieu, we extracted RNAs in the culture medium (CM) of lung adenocarcinoma cells. We next investigated the existing pattern of extracellular lncCRLA. The levels of lncCRLA in CMs of mesenchymal-like A549 and H522 cells were unchanged upon RNase treatment but significantly decreased when treated with RNase and Triton X-100 simultaneously (Fig. 2A), indicating that extracellular lncCRLA was principally wrapped by membrane instead of being directly released. Herein, extracellular exosomes might be obligated to wrap RNA in CM. We then purified exosomes from CM and confirmed their identity by the exosome markers TSG101 and CD9 (Fig. S2A). Exosomes isolated from mesenchymal-like and epithelial-like A549 cells and H522 cells exhibited similar cup-shaped morphology, size, and number (Fig. 2B and S2B). As expected, exosomal lncCRLA levels were significantly higher in the mesenchymal-like A549 and H522 cells than those in epithelial-like cells (Fig. 2C). As shown in Fig. S2C, lncCRLA was specifically packaged in the exosomes of mesenchymal-like tumor cells.

Cell-secreted exosomes and capped cargoes can be internalized by neighboring cells [15,16]. Intracellular lncCRLA was increased upon incubation with exosomes from mesenchymal-like tumor cells, but not lncCRLA-knockout mesenchymal-like tumor cells (Fig. 2D and S2D). Epithelial-like recipient cells showed no difference in uptake efficiency of exosomes of different origins (Fig. 2E and S2E). The increase of lncCRLA levels in epithelial-like recipient cells was not affected by RNA polymerase II inhibitor, actinomycin D, excluding the involvement of endogenous induction (Fig. 2F and S2F). To further confirm that lncCRLA was transferred to recipient cells (epithelial-like tumor cells) via exosomes, we electroporated mesenchymal-like A549 and H522 cells with fluorescein isothiocyanate (FITC)-lncCRLA, and exosomes were isolated and labeled with Dil. After incubation with labeled exosomes, co-localization of FITC and Dil was observed in most recipient cells, whereas no internalization of naked FITC-lncCRLA was found in recipient cells (Fig. 2G and S2G). Intercellular transferring of lncCRLA was supported by the observation that lncCRLA was expressed in the *p*-Casp8-negative zone of lung adenocarcinoma tissues (Fig. 2H). In sum, exosomal lncCRLA was secreted and released in the exosomes of mesenchymal-like lung adenocarcinoma and transferred intercellularly.

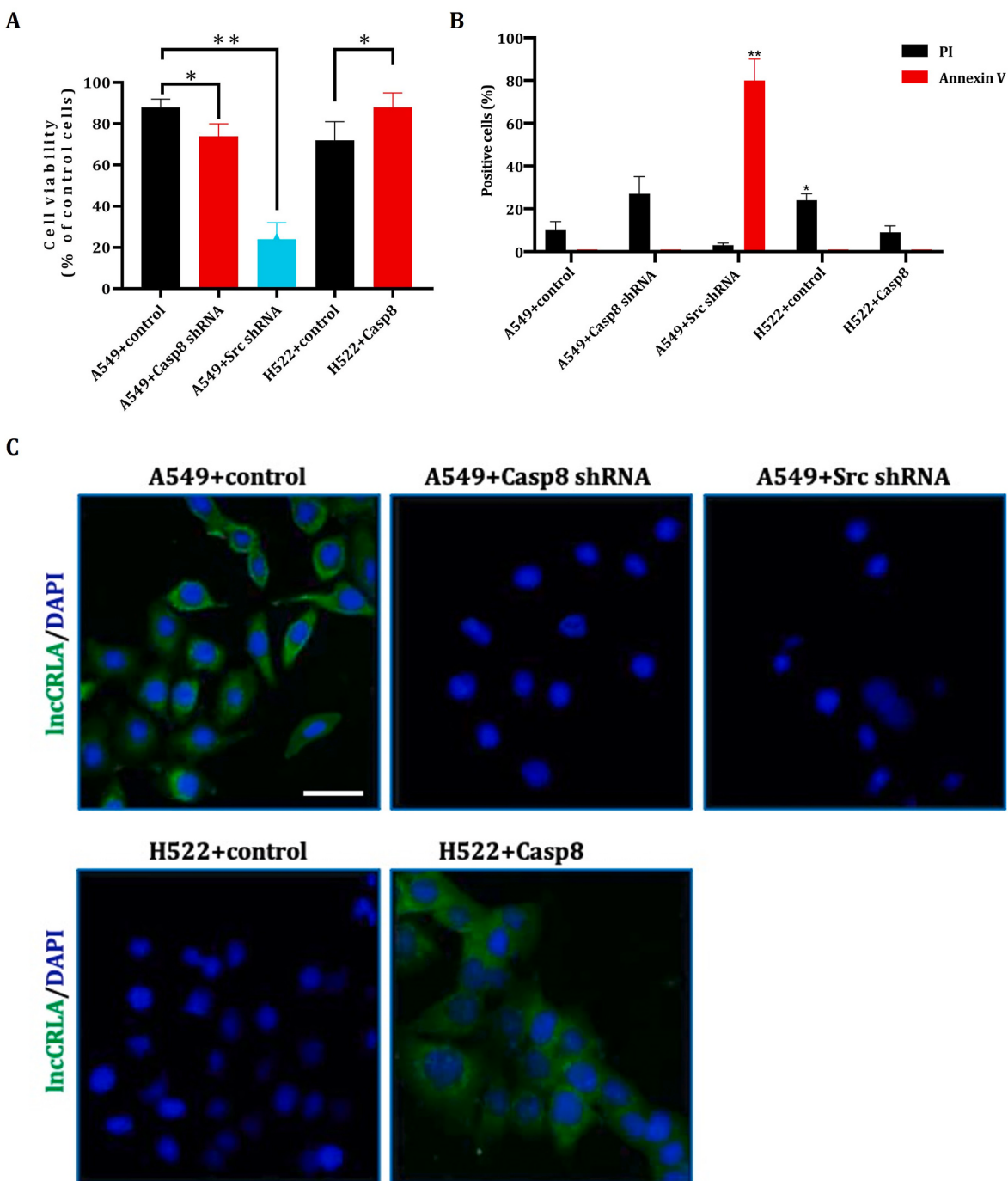


Fig. 1. IncCRLA is highly expressed in the mesenchymal-like lung adenocarcinoma cells.

A, Cell viability is determined by measuring ATP levels using Cell Titer-Glo kit. A549 and H522 cells as indicated are treated with 200 nM paclitaxel for 48 h. Data are represented as mean \pm standard deviation of duplicates. *, $p < 0.05$. **, $p < 0.01$.

B, Annexin V/PI staining by flow cytometry analyzed A549 and H522 cells treated by 200 nM paclitaxel for 48 h ($n = 3$). *, $p < 0.05$. **, $p < 0.01$.

2.1.3. Exosomal IncCRLA from the mesenchymal-like lung adenocarcinoma is unable to alter paclitaxel-induced cell death

Next, we further examined whether intercellularly transferred IncCRLA could confer the resistance to paclitaxel in the epithelial-like tumor cells. The diverse exosomes from mesenchymal/epithelial-like tumor cells were poured into the culture medium of different tumor cells treated with paclitaxel (Fig. 3A). Surprisingly, exosomal IncCRLA from the mesenchymal-like lung adenocarcinoma cells did not affect the paclitaxel-induced cell death percentage and modality in the recipient cells, the epithelial-like lung adenocarcinoma cells (Fig. 3B 3C and S3A).

To dissect the role of exosomal IncCRLA, IncCRLA-lacking exosomes yielded by the epithelial-like cells were electroporated with IncCRLA. The electroporated IncCRLA did not affect the physical properties of the exosomes (Fig. S3B). Then, we explored the role of forcedly expressed IncCRLA in exosomes on the tumoricidal effect of paclitaxel in lung adenocarcinoma cells. Following the addition of exosomes electroporated by IncCRLA, the epithelial-like A549 and H522 cells showed no difference in the tumoricidal effect of paclitaxel with the similar uptake efficiency of exosomes and intracellular increase of IncCRLA (Fig. 3D S3C S3D and S3E). In particular, paclitaxel-induced necroptosis was not

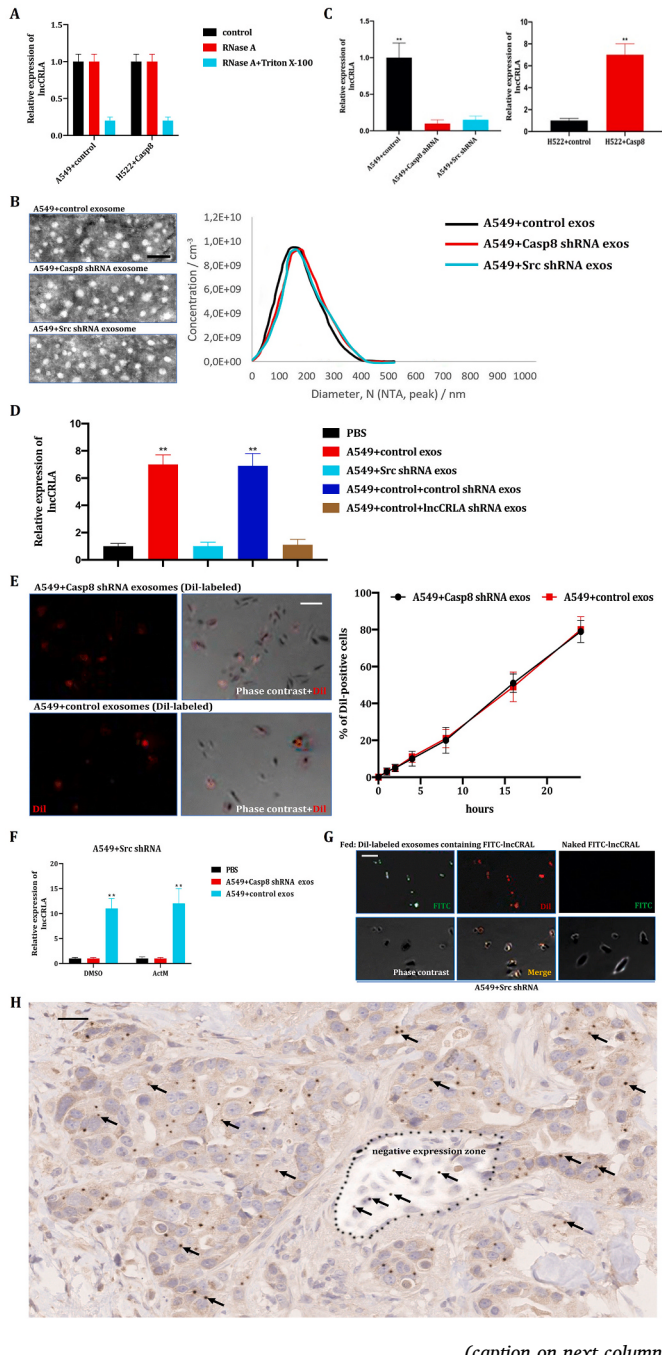


Fig. 2. Exosomal lncCRLA from mesenchymal-like lung adenocarcinoma cells is secreted and intercellularly transferred.

A, qRT-PCR analysis of lncCRLA in the CMs of A549+control and H522+Casp8 cells treated with RNase (2 mg/ml) alone or combined with Triton X-100 (0.1 %) for 20 min (n = 3).

B, Left: representative electron microscopy images of exosomes secreted by A549 cells. Scale bar = 100 nm. Right: NanoSight particle-tracking analysis of the size distributions and number of exosomes.

C, qRT-PCR analysis of lncCRLA in exosomes isolated from the CMs of A549 and H522 cells (n = 3).

D, qRT-PCR analysis of lncCRLA in A549+Casp8 shRNA cells at 48 h after incubation with indicated exosomes (or PBS as control) (n = 3).

E, Left: fluorescent observation of A549+Src shRNA cells incubated with indicated Dil-labeled (red) exosomes for 48 h. Representative fluorescent images and phase contrast images are shown. Scale bar = 500 μ m. Right: Flow cytometry analysis of Dil-positive A549+Src shRNA cells after incubation with Dil-labeled exosomes for indicated time.

F, qRT-PCR analysis of lncCRLA in A549+Src cells treated with Actinomycin D (ActD, 1 μ g/mL) followed by indicated exosomes treatment for 48 h (n = 3). G, Fluorescent observation of A549+Src shRNA cells at 48 h after incubation with Dil-labeled (red) exosomes derived from FITC-lncCRLA (green) electroporated A549+control or naked FITC-lncCRLA. Representative fluorescent images and phase contrast images are shown. Scale bar = 500 μ m

H, Immunohistochemical staining for p-Casp8 and LNA of lncCRLA in lung adenocarcinoma tissues. Scale bar = 50 μ m.

obviously attenuated with the increase of intracellular lncCRLA in the Caspase-8-deficient A549 and H522 cells. To dissect the role of exosomal lncCRLA on cell death in lung adenocarcinoma, we forced lncCRLA to be upregulated in the Caspase-8-lacking A549 and H522 cells. Consistent with our previous report [10], intracellularly upregulated lncCRLA hampered the necrotic cell deaths triggered by paclitaxel in the Caspase-8-lacking A549 and H522 cells (Fig. 3E and F).

We next investigated the underlying mechanism for the incapability of exosomal lncCRLA derived from tumor cells to block necrosis following paclitaxel treatment. We previously reported that RIPK1 was encapsulated in the exosomes from A549 and H522 cells, as well as binding of lncCRLA to RIPK1 in exosomes restricted its suppressive effects on the necrosis in the recipient cells [10]. Accordingly, RIPK1 depletion using CRISPR/CAS9 in the mesenchymal-like A549 cells (A549^{RIPK1-/-}) did not affect the exosomes distribution and exosomal lncCRLA level (Fig. S3F S3G S3H and S3I). A549^{RIPK1-/-} exosomes rescued Caspase-8-deficient A549 cells (A549+Casp8 shRNA) from the paclitaxel-induced necrosis (Figs. S3J and S3K). RIP assay showed that exosomal lncCRLA was totally binding to RIPK1 (Fig. 3G). To further confirm the role of lncCRLA, we electroporated the exosomes from lncCRLA-lacking A549^{RIPK1-/-}+ Casp8/Src shRNA with extracellular lncCRLA (Figs. S3L and S3M). Following the electroporation and transferring of lncCRLA, the intracellular lncCRLA was significantly heightened (Figs. S3N and S3O). The exosomal lncCRLA from A549^{RIPK1-/-}+ Casp8/Src shRNA rescued 10 % of A549+Casp8 shRNA cells from necrosis under paclitaxel intervention (Fig. S3P S3Q and S3R). Together, exosomal lncCRLA harbored a lesser contribution to the therapeutic resistance of paclitaxel in Caspase-8-deficient lung adenocarcinoma cells due to its binding to exosomal RIPK1.

2.1.4. Plasmatic lncCRLA is well-suitedly predictive for the chemotherapy response and progression of lung adenocarcinoma

Our previous study exhibited that p-Casp8 was a precise biomarker to reflect EMT phenotype and resistance to TP regimen (paclitaxel and cisplatin) in lung adenocarcinomas [11]. lncCRLA was expressed and released into extracellular space during p-Casp8-induced EMT [11]. Then, we explored whether exosomal lncCRLA functioned as a biomarker for the diagnosis and treatment of lung adenocarcinoma. p-Casp8 was positively associated with tissue lncCRLA and EMT phenotype [downregulation-Vimentin (Vim, mesenchymal marker) and upregulation-E-cadherin (E-cad, epithelial marker)] in lung

(caption on next column)

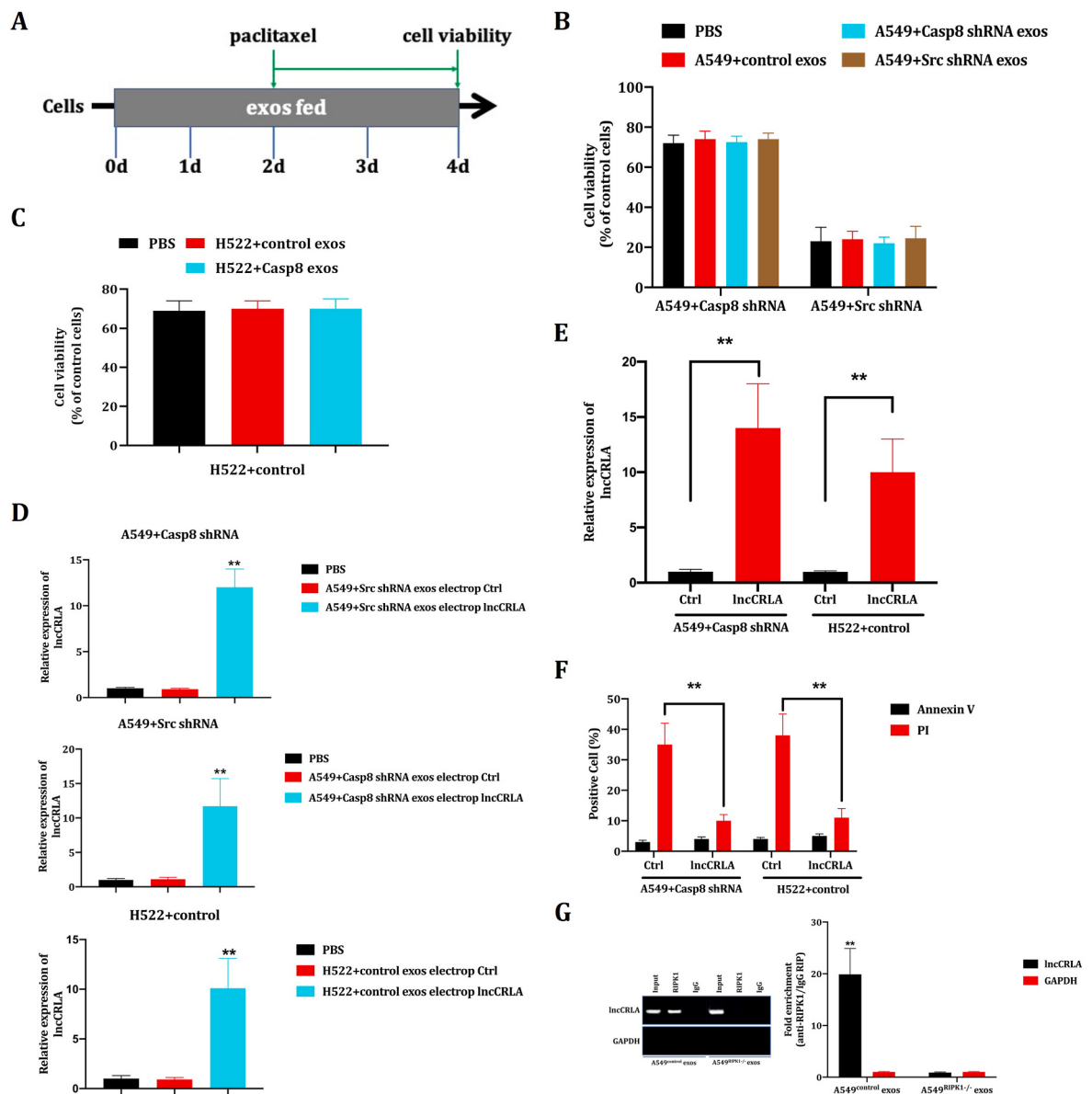


Fig. 3. Exosomal lncCRLA from the mesenchymal-like lung adenocarcinoma is unable to alter paclitaxel-induced cell death.

A, Schematic diagram for the intervention of exosomes and paclitaxel.

B, Cell viability of A549+Casp8/Src shRNA cells pre-incubated with indicated exosomes (or PBS as control) for 48 h followed by paclitaxel treatment for 48 h ($n = 3$).

C, Cell viability of H522+control cells pre-incubated with indicated exosomes (or PBS as control) for 48 h followed by paclitaxel treatment for 48 h ($n = 3$).

D, qRT-PCR analysis of lncCRLA in A549 and H522 cells fed with exosomes electroporated by control and lncCRLA for 48 h ($n = 3$). **, $p < 0.01$.

E, qRT-PCR analysis of lncCRLA in A549+Casp8 shRNA and H522+control cells fed with exosomes electroporated by control and lncCRLA for 48 h ($n = 3$). **, $p < 0.01$.

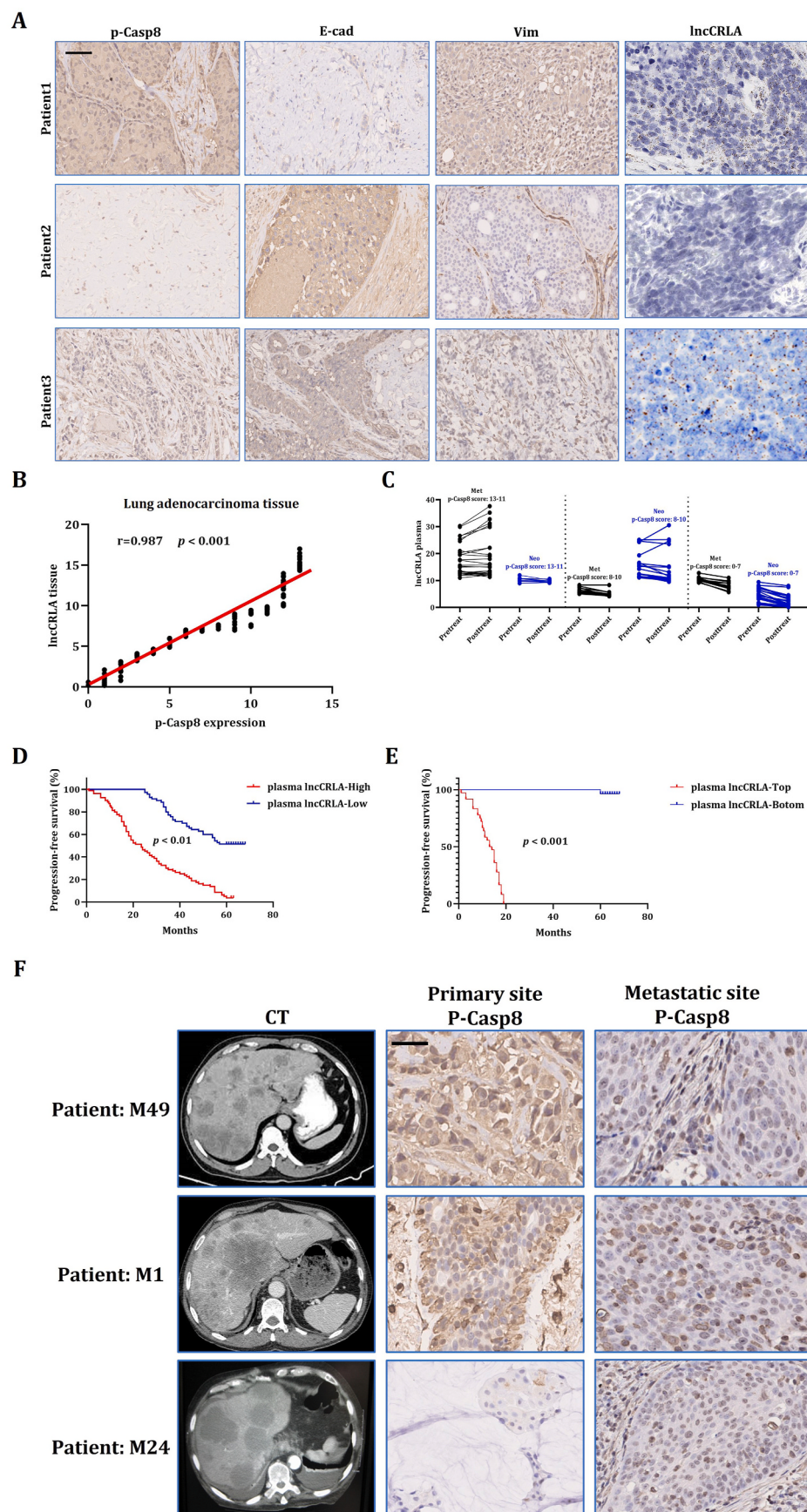
F, Annexin V/PI staining by flow cytometry analyzes A549+Casp8 shRNA and H522+control cells fed with exosomes electroporated by control and lncCRLA followed by paclitaxel treatment for 48 h ($n = 3$). **, $p < 0.01$.

G, Left: gel electrophoresis of PCR products from RIP assay. Right: RIP assay of the enrichment of anti-RIPK1 on lncCRLA relative to IgG in the exosomal lysates of indicated cells ($n = 3$). **, $p < 0.01$.

adenocarcinoma tissues (Fig. 4A). *p*-Casp8 immunohistochemistry (IHC) score was tightly correlated with tissue lncCRLA in lung adenocarcinomas (Fig. 4B and S4A). To further examine whether lncCRLA was present in extracellular milieu, we extracted exosomal RNAs in the plasmas of patients with lung adenocarcinoma. The correlation between tissue and plasmatic lncCRLA was corroborated in the patients with lung adenocarcinoma (Fig. S4B).

Next, we explored whether circulating lncCRLA was potential to predict chemotherapy response to TP regimen in lung adenocarcinoma patients. 121 participants were involved, including 68 patients with operable lung adenocarcinoma receiving neoadjuvant chemotherapy

and 53 patients with metastatic lung adenocarcinoma receiving palliative chemotherapy (Table S1). The average level of lncCRLA in pre-therapy plasma was lower in patients who suffered from complete response (CR) compared with those who suffered from partial response (PR), stable disease (SD) and progressive disease (PD) (Figs. S4C and S4D). Both early- and terminal-stage patients were divided into two groups referring to plasmatic lncCRLA, high and low lncCRLA group (lncCRLA-high and lncCRLA-low). Both early- and terminal-stage patients with low lncCRLA in the pre-therapy plasma obtained the higher objective response and CR rate to TP regimen (Figs. S4E and S4F). Circulating lncCRLA was able to consistently reflect the response of TP



(caption on next page)

- Fig. 4.** Plasmatic lncCRLA is well-suitedly predictive for the chemotherapy response and progression of lung adenocarcinoma.
 A, LNA ISH of lncCRLA and immunostaining of p-Casp8, E-cad and Vim in the consecutive tumor sections from human lung adenocarcinoma. Scale bar = 100 μm
 B, Pearson correlation analysis between tissue lncCRLA and p-Casp8 expression in lung adenocarcinoma tissues
 C, qRT-PCR analysis of lncCRLA in the plasma of lung adenocarcinoma patients before and after TP regimen treatment with different p-Casp8 IHC score.
 D, Kaplan-Meier analysis of PFS in resectable lung adenocarcinoma patients with low and high level of plasmatic lncCRLA.
 E, Kaplan-Meier analysis of PFS in resectable lung adenocarcinoma patients with top (10 %) and bottom (10 %) level of plasmatic lncCRLA.
 F, Immunostaining of p-Casp8 in the metastatic sites from resectable lung adenocarcinoma patients presenting CT scanning.

regimen in lung adenocarcinoma patients (Figs. S4G and S4H). Moreover, postoperative plasmatic lncCRLA was significantly attenuated in the patients with resectable lung adenocarcinoma regardless of p-Casp8 expression (Fig. S4I). lncCRLA in the plasmas of lung adenocarcinoma patients mirrored the clinical therapeutic effect in the lung adenocarcinoma patients with different p-Casp8 expressions (Fig. 4C S4G and S4H). Collectively, plasmatic lncCRLA represented the therapeutic effect of TP regimen in lung adenocarcinoma. Collective, plasmatic lncCRLA functioned as an optimized predictor for chemotherapy response and metastasis of lung adenocarcinoma.

Then, we analyzed the correlation between plasmatic lncCRLA and disease progression in lung adenocarcinoma patients with neoadjuvant chemotherapy. TP regimen provided the superior benefit to the progression-free survival (PFS) of patients with low plasmatic lncCRLA as compared with those with high plasmatic lncCRLA (Fig. 4D). There was a remarkable divergence in the PFS of lung adenocarcinoma patients with top (10 %) and bottom (10 %) expression of lncCRLA (Fig. 4E). Consistently, lower level of plasmatic lncCRLA provided a substantial benefit of the PFS in the cohort with metastatic lung adenocarcinoma (Fig. S4J). In order to disclose the role of lncCRLA on disease progression, plasmatic lncCRLA was repeatedly tested as shown in Fig. S4K. It was intriguing that metastasis arose in 8 resectable lung adenocarcinomas with postoperative plasmatic lncCRLA of >0.5 during 18 months after operation, in which 3 cases occurred in the p-Casp8-low lung adenocarcinoma (Table S2).

It was noteworthy that plasmatic lncCRLA in patients with metastatic disease was relatively higher than that in those with early-stage diseases (neoadjuvant chemotherapy) (Figs. S4C and S4D). The larger proportion of patients with metastatic lung adenocarcinoma presented the p-Casp8-high and plasmatic lncCRLA-high (Fig. S4L). The plasmatic lncCRLA and p-Casp8 in the metastatic sites were coordinated in the patients with postoperative metastasis regardless of p-Casp8 expression in the primary sites (Figs. S4M and S4N). Patients with lung adenocarcinoma metastasis yielded the similar prognosis on the behalf of PFS regardless of p-Casp8 expression in the primary sites (Fig. S4O). In 18 cases of lung adenocarcinoma patients with hepatic metastasis, p-Casp8 in the metastatic sites was vigorously expressed, even in the p-Casp8-negative primary site (score:0–1, Fig. 4F). The higher lncCRLA level in patients with metastatic lung adenocarcinoma presumably resulted from the release of lncCRLA from p-Casp8-positive metastatic sites.

2.1.5. lncCRLA-expressing hybrid EMT cells are the origin to lung adenocarcinoma by single-cell RNA-seq and spatial transcriptomics

Mounting evidence indicated that EMT and the reverse process, mesenchymal-epithelial transition (MET), accounted for heterogeneity and evolvement of human tumor [8,9]. lncCRLA was a novel biomarker for EMT of lung adenocarcinoma. Was lncCRLA able to characterize the heterogeneity of EMT state in lung adenocarcinoma? It was uncovered that E-cad and Vim were heterogeneously expressed among lung adenocarcinomas, both of which were negatively correlated (Fig. 5A). Even in the same individual sections, E-cad and Vim were heterogeneous in the distinct regions (Fig. S5A). It indicated that the heterogeneity of EMT of lung adenocarcinoma was ubiquitous. To further disclose EMT state in lung adenocarcinoma, we defined the epithelial (E) state, mesenchymal (M) state and hybrid EMT state as E-cad⁺Vim⁻, E-cad⁺Vim⁺ and E-cad⁺Vim⁺, respectively. We designed the gating strategy to discrete the tumor cells from epithelial/mesenchymal/hybrid EMT state by flow cytometry in the resectable lung adenocarcinomas (Fig. S5B). Next, we

sought for the relationship between plasmatic lncCRLA and EMT phenotype. The proportions of tumor cells with mesenchymal state and hybrid EMT state in lncCRLA-high lung adenocarcinoma were obviously higher than those in lncCRLA-low lung adenocarcinomas (Fig. S5C), while lncCRLA-low lung adenocarcinoma dominantly preferred to epithelial phenotype (Fig. S5C). Compared with epithelial phenotype, mesenchymal and hybrid EMT phenotypes were positively correlated with plasmatic lncCRLA in lung adenocarcinoma patients (Fig. 5B). It inferred that plasmatic lncCRLA was able to mirror EMT phenotype in lung adenocarcinoma. It was noteworthy that EMT heterogeneity and distribution in lung adenocarcinoma tissues did not depend on tumor stage, indicating that EMT phenotype distribution in lung adenocarcinoma might be unchangeable during tumor progression (Fig. S5D). It attracted our attentions to investigate whether plasmatic lncCRLA was potential to reflect the heterogeneity and evolvement of lung adenocarcinoma.

To dissect the relationship between EMT phenotype and lung adenocarcinoma heterogeneity, we applied the single-cell RNA sequencing (scRNA-seq) to analyze the single cell EMT phenotype. 2 early-stage lung adenocarcinomas [1 for lncCRLA-low: 3.1 (N15 Table S1) and 1 for lncCRLA-high: 16.33 (N51 Table S1)] and 1 tumor adjacent tissues corresponding to 3 lung adenocarcinoma patients were pipelined for RNA-seq (Fig. S5E). A conventional workflow was used to isolate viable single cells from surgical resection (Fig. S5F). 11,102 viable cells were isolated from 1 surgical lung adenocarcinoma sample with plasmatic lncCRLA-low. All viable cells were discriminated into the various clusters with tumor cells and immune cells (Fig. 5C). Given the high dimensionality, canonical EMT markers, E-cad and Vim, were selected for principal analysis. According to EMT markers, tumor cells were divided into the epithelial, hybrid EMT and mesenchymal populations (Fig. S5G). Surprisingly, hybrid EMT cells took a major part in lncCRLA-low lung adenocarcinoma (Fig. S5G). Using the clustering analysis, we identified epithelial, hybrid EMT and mesenchymal populations with different gene expression profiles (Fig. S5H). Heatmap of clusters with EMT states revealed the between-state heterogeneity (Fig. S5H). Specifically, EMT subpopulations had the different signaling enrichment (Fig. S5I). The most differently expressed genes were subjected to validation in the EMT subpopulations (Fig. S5J). Subsequently, we re-tested our concept in lncCRLA-high lung adenocarcinoma. 10,111 viable cells were obtained from 1 surgical lung adenocarcinoma sample with plasmatic lncCRLA-high (Fig. S5K). Hybrid EMT cells also took a major part relative to epithelial or mesenchymal cells portion (Fig. S5L). Different states of tumor cells presented the heterogeneity by heatmap of clusters (Figs. S5M and S5N). Together, EMT phenotype reflected the heterogeneity of lung adenocarcinoma.

In an attempt to track tumor evolvement in the background of EMT dynamic, we further analyzed the mRNA of single tumor cell to define as the nonsynonymous single-nucleotide variants and copy-number alterations by RNA-MuTect assay [17,18]. Owing to the large-scale chromosomal alterations in human cancer, we utilized the copy number variation from mRNAs to discriminate epithelial cells from cancer to non-cancer (Figs. S5O and S5P). To detect somatic mutations from bulk RNA-seq data (Table S3) to unravel the tumor evolvement, RNA-MuTect was utilized to analyze this type of data. Terminally, hybrid EMT cells preferred to distribute to the trunk clonal in lung adenocarcinoma cells with low or high plasmatic lncCRLA (Fig. 5D). A handful of hybrid EMT cells resided at the top of lung adenocarcinoma evolvement track (Fig. 5D). It was of notes that hybrid EMT cells from trunk clone were

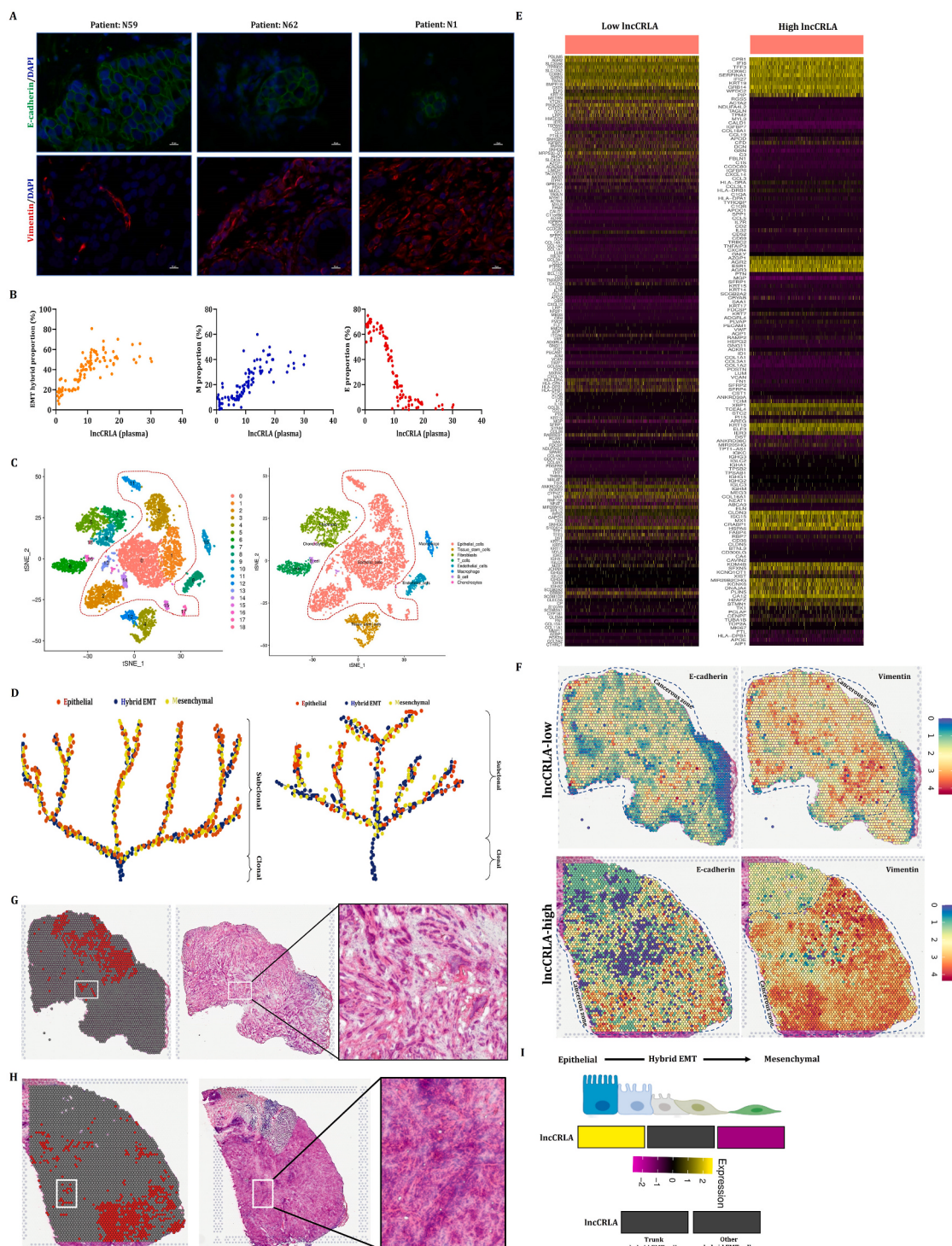


Fig. 5. IncCRLA-expressing hybrid EMT cells are the origin to lung adenocarcinoma by single-cell and spatial transcriptomics.

A, Fluorescence images of E-cadherin and Vimentin in lung adenocarcinoma tissues. Scale bar = 10 μm

B, Flow cytometry analysis for epithelial (E)/mesenchymal (M)/hybrid state cells and correlation between EMT phenotype and plasmatic IncCRLA.

C, t-stochastic neighbor embedding (t-SNE) plot of all cells from lung adenocarcinoma with plasmatic IncCRLA-low colored by their cellular identity (epithelial cells [n = 4012], immune cells [n = 5129], stromal cells [n = 1961]).

D, Potential trajectory of all cancer cells identified three distinct cell states colored by cluster as indicated according to RNA-MuTect in IncCRLA-low (left)/high (right) tumor samples. The clonal-subclonal showed the potential evolutionary direction in the trajectory.

E, Heatmap showing clustered into hybrid EMT profiles in IncCRLA-low/high lung adenocarcinoma. Color key differentially coding from yellow to red indicated the relative expression level from low to high.

F, Mapped with unbiased E-cadherin/Vimentin clustering of spatial transcriptomics spots in IncCRLA-low (upper)/high (lower) tumor samples. Cancerous region is surrounded by dotted.

G, H&E staining of tissue section representing ST spot in IncCRLA-low lung adenocarcinoma (Fig. 5G). Box indicates hybrid EMT cells from trunk clone (Fig. 5E).

H, H&E staining of tissue section representing ST spot in IncCRLA-high lung adenocarcinoma (Fig. 5H). Box indicates hybrid EMT cells from trunk clone (Fig. 5E).

I, sc-RNA seq indicated IncCRLA expression in distinct EMT cell.

indiscriminated from other hybrid EMT cells on the basis of bulk scRNA-seq (Fig. 5E). We applied the spatial transcriptomics to disclose the spatial distribution of lung adenocarcinoma cells with different EMT phenotypes. Lung adenocarcinoma cells with different EMT phenotypes distributed with the complex pattern (Fig. 5F). The phylogenetic tree generally recapitulated the geographic origin of lung adenocarcinoma. Trunk hybrid EMT cells located in the section of lung adenocarcinomas according to spatial transcriptomics (Fig. 5G and H). Remarkably, lncCRLA level was significantly differed among 3 EMT subpopulations (Fig. 5I), while it was similar between trunk and other hybrid EMT cells (Fig. 5I). Collectively, trunk hybrid EMT cells with increased lncCRLA were characterized to initiate lung adenocarcinoma, inferring the possibility that plasmatic lncCRLA predicted the initiation of lung adenocarcinoma.

2.1.6. lncCRLA is a well-suited predictor for the preinvasive lesion of lung adenocarcinoma

Next, we explored whether lncCRLA was released into circulation as a plasmatic biomarker for early detection by trunk hybrid EMT cells. We constructed the brand-new mouse model to clarify the role of lncCRLA on the evolution of lung adenocarcinoma. To generate tumors sporadically in the lungs of K-ras^{LSL-G12D} mice, our team initially used replication-deficient adeno-viruses expressing Cre (Ad-Cre) to deliver transient Cre expression to infect cells of the lung [13,19–21]. Basically, we generated the brand-new mouse model with both conditional K-ras^{LSL-G12D/+} and c-Src^{Y527A}, in which lung adenocarcinoma was more aggressive with c-Src overactivation (*p*-Src) and Caspase-8 phosphorylation (*p*-Casp8, Fig. S6A). To trace EMT process, double immunofluorescent markers, epithelial ZsGreen and mesenchymal tdTomato, were introduced into the mouse model as shown in Fig. 6A. After profiling the mouse genomics, we did not match the isogenic lncRNA to human lncCRLA. Wnt signaling played a crucial role on *p*-Casp8-induced EMT in the mice [10,22,23]. Herein, human lncCRLA sequence with mouse Wnt promotor were constructed to detect the association between the onset of lung adenocarcinoma and plasmatic lncCRLA expression (Fig. 6A).

Subsequently, lung adenocarcinogenesis was observed in the conditional mouse model after adenoCre administration (Fig. 6A) [19]. As the result of the preliminary data, the histopathological progression was summarized in Table S4. The different groups of mice were analyzed at post-infection 3, 6, 9 and 12 weeks, respectively. In our mouse model, the incidence of lung adenocarcinoma was approximately 100 %. 12 weeks were taken from benign lesion (adenoma), preinvasive lesions (atypical adenomatous hyperplasia/adenocarcinoma *in situ*), lung adenocarcinoma to metastatic lung adenocarcinoma (Fig. 6B). Moreover, we were sought for the expressions of *p*-Src and *p*-Casp8 in preinvasive lesions and lung adenocarcinoma. In the context of c-Src activation, lower level of *p*-Casp8 was expressed in the atypical adenomatous hyperplasia compared with that in lung adenocarcinoma (Fig. S6A). A slight number of cells showed hybrid EMT phenotype with mesenchymal tdTomato in the atypical adenomatous hyperplasia (Fig. 6C). Meanwhile, those cells with hybrid EMT phenotype presented malignant characteristics in the specimen of atypical adenomatous hyperplasia (Fig. 6D). By contrast, EMT phenotypes were ubiquitous and mixed in the mouse lung adenocarcinoma (Fig. S6B). Collectively, it indicated that EMT occurred at the preinvasive stage of lung adenocarcinoma, and the cells with hybrid EMT phenotype in the preinvasive lesion of lung might evolve into distinctive cells with varying EMT phenotype.

Subsequently, we expected to find out whether plasmatic lncCRLA was predictive for the adenocarcinogenesis of lung at the early stage of EMT process. lncCRLA in the rodent plasma was significant higher in the stage of atypical adenomatous hyperplasia/adenocarcinoma *in situ* as compared to that at 0 week (Fig. S6C). Apart from that, the level of lncCRLA was higher in the plasma of mouse with lung adenocarcinoma relative to those in the mouse with the atypical adenomatous hyperplasia/adenocarcinoma *in situ* (Fig. S6C). To further confirm the clinical

value of plasmatic lncCRLA in the lung adenocarcinogenesis, we showed the levels of plasmatic lncCRLA in healthy population and patients with lung adenocarcinoma. We consecutively tested the plasmatic lncCRLA from 1021 healthy people with or without smoking history (Table S5). lncCRLA level in healthy population plasma was undetected relative to those with lung adenocarcinoma (Fig. S6D). Pulmonary nodules were found in 278 participants, out of which 18 participants' plasmatic lncCRLAs were detected in the significantly higher level. 10 participants with elevated plasmatic lncCRLA received the pulmonary nodule resection (Table S6), as well as 2 participants with normal lncCRLA level performed pulmonary nodule resection (Table S6). Intriguingly, the postoperative histopathology presented early-stage lung adenocarcinoma in 3 participants with lncCRLA of >1.0 (Table S6 and Fig. S6D). As well, 7 participants with lncCRLA of 0.5–1.0 underwent pulmonary operation and confirmed preinvasive lesion of lung, atypical adenomatous hyperplasia and adenocarcinoma *in situ* (Table S6 and Fig. S6D). In parallel, another 2 cases with normal plasmatic lncCRLA level were nonneoplastic lesion after pulmonary nodule operation (Table S6). Referring to our observations, 0.5 would be defined as the cutoff value to determine the arise of preinvasive lesion of lung. To further interrogate the role of lncCRLA on the tumorigenesis, we preventively administered c-Src inhibitor, dasatinib, that abrogate the c-Src-Caspase-8-mediated EMT to decrease circulating lncCRLA in mouse model. Accordingly, dasatinib efficiently intercepted the adenocarcinogenesis of lung and reduced circulating lncCRLA in the mouse model (Fig. S6F). Collectively, lncCRLA was valuable to predict the onset of lung adenocarcinoma, while dasatinib was potential to prevent lung adenocarcinogenesis at the early stage.

4. Discussion

Our team uncovered that lncCRLA was highly expressed in the mesenchymal-like lung adenocarcinoma cells. lncCRLA was associated with chemotherapy resistance in lung adenocarcinoma with mesenchymal or hybrid EMT state. lncCRLA could be released into intercellular media and transferred by exosomes from mesenchymal-like cells to epithelial-like cells. The plasmatic lncCRLA functioned as the preferred biomarker to reflect the response to chemotherapy and disease progression in lung adenocarcinoma. Through sing-cell sequencing, RNA-Mutect and spatial transcriptomics, a bunch of hybrid EMT cells were characterized as the origin from lung adenocarcinoma, which were indiscriminated from hybrid EMT cells with elevated lncCRLA by in-depth single-cell sequencing. Plasmatic lncCRLA was properly predictive for the preinvasive lesion of human lung. Subsequently, the brand-new transgenic mouse model was constructed in which EMT was tracked by Cre and Dre system. In the mouse model, lncCRLA level was elevated in the preinvasive lesion of lung (Fig. 7). Dasatinib was potential to intercept the progression from preinvasive to invasive lesion of mouse lung.

Tumoricidal mechanisms of chemotherapy drugs were substantially diverse and complex [24]. However, chemotherapy-induced cell death pathways were enumerably terminated. Studies over the past decades have explored the functions and consequences of cellular demise and elucidated the key cell death pathways [25]. The chemotherapy-induced cell death sensing machinery was still a riddle. Our findings indicated likelihood that FADD-c-FLIP complex functions as the sensor to initiate the intracellular cell death pathways, especially for paclitaxel. That notion was confirmed by targeted drug in the non-small cell lung cancer [26]. Apoptosis and necrosis were leveraged by the complex of FADD-c-FLIP-Casp8-RIPK1 following the paclitaxel treatment in lung adenocarcinoma. Caspase-8 was a crux between EMT and cell death in lung adenocarcinoma [24]. Phosphorylated Caspase-8 by c-Src was depicted as a major obstacle for therapeutic drugs and EMT process in lung adenocarcinoma. lncCRLA was expressed during *p*-Casp8-induced EMT in lung adenocarcinoma.

Whether intrinsic or acquired, lncRNAs played a critical role on the

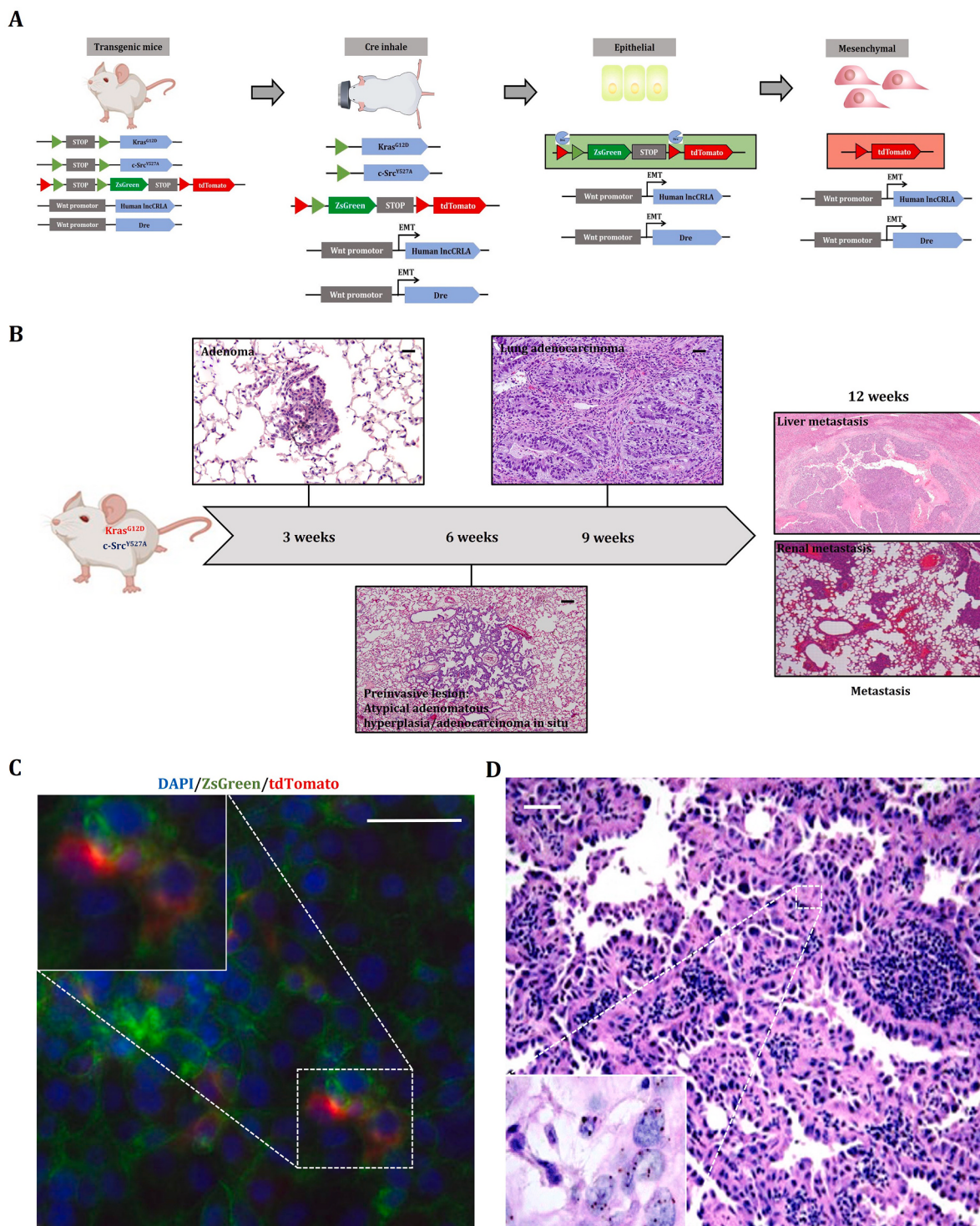


Fig. 6. IncCRLA is a well-suited predictor for the preinvasive lesion of lung adenocarcinoma.

A, Schematic showing strategy for Cre-loxP mediated Dre generation and subsequent Dre-rox recombination that switches ZsGreen to tdTomato in the transgenic mice as indicated. After c-Src-Casp8 interaction, constitutive Dre recombinase genotype is generated and driven by EMT gene Wnt promoter to monitor transient EMT gene activity. After EMT induction, the system would switch ZsGreen to tdTomato labeling on tumor cells that have expressed EMT marker gene (Dre recombinase).

B, Schematic diagram of the onset and development of lung adenocarcinoma in the mouse model. Representative histopathological photos are showed. Scale bar = 50 μ m

C, Immunofluorescence for tdTomato, ZsGreen and DAPI in the lung atypical adenomatous hyperplasia sections. Box indicates mixed fluorescence zone. Scale bar = 50 μ m.

D, H&E staining of mouse lung atypical adenomatous hyperplasia. Box indicates cells with malignant characteristics. Scale bar = 50 μ m.

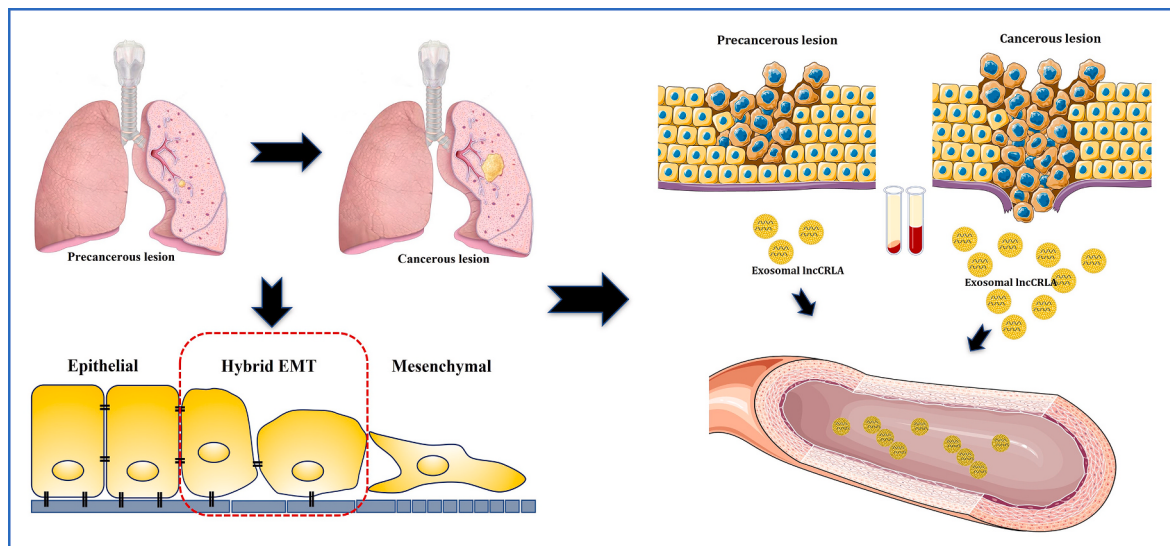


Fig. 7. Graphical abstract showing the predictive role of plasmatic lncCRLA.

chemoresistance [27]. Our previous study indicated that lncCRLA attenuated paclitaxel-induced necroptosis in apoptosis-blocking lung adenocarcinoma cells (Casp8 depletion or phosphorylation) [10]. According to our observations, exosomal lncCRLA was unable to extend chemoresistance to paclitaxel in lung adenocarcinoma owing to the binding of lncCRLA to RIPK1 in exosomes. However, lncCRLA was released into intercellular milieu as plasmatic biomarker. A bunch of lncRNAs were released into circulation as circulating biomarker to reflect tumor biological phenotypes [28]. As fact, lncRNAs were potential to function as predictors for disease progression and occurrence due to PCR's high sensitivity [15,29]. On the basis of our data, lncCRLA was able to play a critical role in predicting lung adenocarcinoma progression and recurrence. lncCRLA testing presented high sensitivity and accuracy. It shed a slight light on its clinical practice.

The recent mounting evidences indicated hybrid EMT was critical for tumor development and therapeutic resistance [9,30,31]. Hybrid EMT cells did great efforts on tumor metastasis, chemotherapy resistance and plasticity [32–34]. EMT *in vivo* was transient and dynamic in the carcinogenesis process, which remains technically hard to capture at the real time [8,21,35]. The genomes of cancer cells were littered with mutations, some of which might contribute to growth of the cancer by activating tumor-promoting genes called oncogenes, or by switching off genes belonging to a class known as tumor suppressors [36]. Spatial and single-cell dissection of the genomic changes occurring during the evolution of human non-small cell lung cancer may help elucidate the basis for its dismal prognosis [37,38]. Single-cell sequencing technology did a favor to increasingly understand the subpopulation details of immune cells in lung adenocarcinoma [39–41]. We define the trunk hybrid EMT cells as origin of lung adenocarcinoma. Nevertheless, those original cells of lung adenocarcinoma with high expression of lncCRLA cannot be characterized by the deep single-cell sequencing. It was more likely that plasmatic lncCRLA was predictive to the occurrence of lung adenocarcinoma. It was difficult to target original tumor cells without well-suited target molecules. Our results were confirmed by Marjanovic's data that high plasticity cells were precursors for lung adenocarcinoma with mesenchymal phenotype [42].

Despite growing efforts for its early detection by screening populations at risk, the majority of lung cancer patients are still diagnosed in an advanced stage [41,43,44]. Predictive biomarkers of lung adenocarcinoma have not dramatically improved in the last decade [41,43]. In our study, plasmatic lncCRLA was valuable for the prediction of lung adenocarcinoma development. We were ought to pay more attention on the populations with circulating lncCRLA of >0.5 and the risk factors of

lung adenocarcinoma. Besides, lncCRLA shed a great light on the prevention of lung adenocarcinoma. Genetically engineered mouse models of human cancer can help to address this gap. In the engineered transgenic mouse models, c-Src inhibitor, dasatinib, was able to intercept the development of lung adenocarcinoma. Therefore, surgery might not be an optimized option for early-stage intervention in the population with pulmonary nodule and elevated lncCRLA. Our data supported the notion that preinvasive tumor could be altered into benign lesion by c-Src inhibitor. Dasatinib might affect the more tyrosine kinases in human, especially for c-Src [45,46]. Dasatinib was not characterized as a potent agent for patients with lung cancer [45,47–49]. No success of dasatinib to patients with lung cancer was ascribed to the population selection. Subsequently, we expected to recruit more people with lung cancer risk to test the sensitivity and accuracy of plasmatic lncCRLA and the dramatically clinical value of dasatinib.

Funding

Supported by National Natural Science Foundation of China (No. 81872390) and YJ (ZD)201,706.

CRediT authorship contribution statement

Shuai Lin: Validation, Formal analysis. **Chenyang He:** Project administration, Methodology, Conceptualization. **Lingqin Song:** Visualization, Validation. **Liangzhang Sun:** Visualization, Formal analysis, Data curation. **Renyang Zhao:** Visualization, Resources, Methodology. **Weili Min:** Validation, Software. **Yang Zhao:** Writing – review & editing, Writing – original draft, Methodology, Investigation, Funding acquisition, Formal analysis, Data curation, Conceptualization.

Declaration of competing interest

The authors declare that they have no known competing financial interests or personal relationships that could have appeared to influence the work reported in this paper.

Acknowledgement

A lot of thanks for doctor Jian Liu who died of non-small cell lung cancer in 2022. He completed a bunch of cell experiments. A lot of thanks for Shanshan Xu who worked in my team as a researcher. Jian Liu and Shanshan Xu requested the anonymity for this paper.

Appendix A. Supplementary data

Supplementary data to this article can be found online at <https://doi.org/10.1016/j.canlet.2023.216588>.

References

- [1] H. Sung, J. Ferlay, R.L. Siegel, M. Laversanne, I. Soerjomataram, A. Jemal, F. Bray, Global cancer statistics 2020: GLOBOCAN estimates of incidence and mortality worldwide for 36 cancers in 185 countries, *Ca - Cancer J. Clin.* (2021).
- [2] R. Zheng, H. Zeng, T. Zuo, S. Zhang, Y. Qiao, Q. Zhou, W. Chen, Lung cancer incidence and mortality in China, *Thorac Cancer* 7 (2016) (2011) 94–99.
- [3] S. Gao, N. Li, S. Wang, F. Zhang, W. Wei, N. Li, N. Bi, Z. Wang, J. He, Lung cancer in people's Republic of China, *J. Thorac. Oncol.* 15 (2020) 1567–1576.
- [4] C. Xia, X. Dong, H. Li, M. Cao, D. Sun, S. He, F. Yang, X. Yan, S. Zhang, N. Li, W. Chen, Cancer statistics in China and United States, 2022: profiles, trends, and determinants, *Chin. Med. J.* 135 (2022) 584–590.
- [5] J.Y. Xu, C. Zhang, X. Wang, L. Zhai, Y. Ma, Y. Mao, K. Qian, C. Sun, Z. Liu, S. Jiang, M. Wang, L. Feng, L. Zhao, P. Liu, B. Wang, X. Zhao, H. Xie, X. Yang, L. Zhao, Y. Chang, J. Jia, X. Wang, Y. Zhang, Y. Wang, Y. Yang, Z. Wu, L. Yang, B. Liu, T. Zhao, S. Ren, A. Sun, Y. Zhao, W. Ying, F. Wang, G. Wang, Y. Zhang, S. Cheng, J. Qin, X. Qian, Y. Wang, J. Li, F. He, T. Xiao, M. Tan, Integrative proteomic characterization of human lung adenocarcinoma, *Cell* 182 (2020) 245–261 e217.
- [6] J. Chen, H. Yang, A.S.M. Teo, L.B. Amer, F.G. Sherbaf, C.Q. Tan, J.J.S. Alvarez, B. Lu, J.Q. Lim, A. Takano, R. Nahar, Y.Y. Lee, C.Z.J. Phua, K.P. Chua, L. Suteja, P. Chen, M.M. Chang, T.P.T. Koh, B.H. Ong, D. Ananthan, A.A.L. Hsu, A. Gogna, C. W. Too, Z.W. Aung, Y.F. Lee, L. Wang, T.K.H. Lim, A. Wilim, P.S. Choi, P.Y. Ng, C. K. Toh, W.T. Lim, S. Ma, B. Lim, J. Liu, W.L. Tam, A.J. Skanderup, J.P.S. Yeong, E. H. Tan, C.L. Creasy, D.S.W. Tan, A.M. Hillmer, W. Zhai, Genomic landscape of lung adenocarcinoma in East Asians, *Nat. Genet.* 52 (2020) 177–186.
- [7] M.B. Nilsson, Y. Yang, S. Heeke, S.A. Patel, A. Poteete, H. Udagawa, Y.Y. Elamin, C. A. Moran, Y. Kashima, T. Arumugam, X. Yu, X. Ren, L. Dia, L. Shen, Q. Wang, M. Zhang, J.P. Robichaux, C. Shi, A.N. Pfeil, H. Tran, D.L. Gibbons, J. Bock, J. Wang, J.D. Minna, S.S. Kobayashi, X. Le, J.V. Heymach, CD70 is a therapeutic target upregulated in EMT-associated EGFR tyrosine kinase inhibitor resistance, *Cancer Cell* 41 (2023) 340–355 e346.
- [8] D.P. Cook, B.C. Vanderhyden, Context specificity of the EMT transcriptional response, *Nat. Commun.* 11 (2020) 2142.
- [9] B. Bakir, A.M. Chiarella, J.R. Pitarresi, A.K. Rustgi, EMT, MET, plasticity, and tumor metastasis, *Trends Cell Biol.* 30 (2020) 764–776.
- [10] W. Min, L. Sun, B. Li, X. Gao, S. Zhang, Y. Zhao, IncCRLA enhanced chemoresistance in lung adenocarcinoma that underwent epithelial-mesenchymal transition, *Oncol. Res.* 28 (2021) 857–872.
- [11] Y. Zhang, L. Sun, X. Gao, A. Guo, Y. Dia, Y. Zhao, RNF43 ubiquitinates and degrades phosphorylated E-cadherin by c-Src to facilitate epithelial-mesenchymal transition in lung adenocarcinoma, *BMC Cancer* 19 (2019) 670.
- [12] W. Lu, Y. Kang, Epithelial-mesenchymal plasticity in cancer progression and metastasis, *Dev. Cell* 49 (2019) 361–374.
- [13] L.G. Karacosta, B. Anchang, N. Ignatiadis, S.C. Kimmy, J.A. Benson, J.B. Shrager, R. Tibshirani, S.C. Bendall, S.K. Plevritis, Mapping lung cancer epithelial-mesenchymal transition states and trajectories with single-cell resolution, *Nat. Commun.* 10 (2019) 5587.
- [14] F. Chemi, D.G. Rothwell, N. McGranahan, S. Gulati, C. Abbosh, S.P. Pearce, C. Zhou, G.A. Wilson, M. Jamal-Hanjani, N. Birkbak, J. Pierce, C.S. Kim, S. Ferdous, D.J. Burt, D. Slane-Tan, F. Gomes, D. Moore, R. Shah, M. Al Bakir, C. Hiley, S. Veeriah, Y. Summers, P. Crosbie, S. Ward, B. Mesquita, M. Dynowski, D. Biswas, J. Tugwood, F. Blackhall, C. Miller, A. Hackshaw, G. Brady, C. Swanton, C. Dive, T. R. Consortium, Pulmonary venous circulating tumor cell dissemination before tumor resection and disease relapse, *Nat. Med.* 25 (2019) 1534–1539.
- [15] I. Keklikoglou, C. Cianciaruso, E. Guc, M.L. Squadrato, L.M. Spring, S. Tazziman, L. Lambein, A. Poissonnier, G.B. Ferraro, C. Baer, A. Cassara, A. Guichard, M. L. Iruela-Arispe, C.E. Lewis, L.M. Coussens, A. Bardia, R.K. Jain, J.W. Pollard, M. De Palma, Chemotherapy elicits pro-metastatic extracellular vesicles in breast cancer models, *Nat. Cell Biol.* 21 (2019) 190–202.
- [16] G. van Niel, G. D'Angelo, G. Raposo, Sheding light on the cell biology of extracellular vesicles, *Nat. Rev. Mol. Cell Biol.* 19 (2018) 213–228.
- [17] A. Taylor-Weiner, C. Stewart, T. Giordano, M. Miller, M. Rosenberg, A. Macbeth, N. Lennon, E. Rheinbay, D.A. Landau, C.J. Wu, G. Getz, DeTiN: overcoming tumor-in-normal contamination, *Nat. Methods* 15 (2018) 531–534.
- [18] K. Yizhak, F. Aguet, J. Kim, J.M. Hess, K. Kubler, J. Grimsby, R. Frazer, H. Zhang, N.J. Haradhvala, D. Rosebrock, D. Livitz, X. Li, E. Arich-Landkof, N. Shores, C. Stewart, A.V. Segre, P.A. Branton, P. Polak, K.G. Ardlie, G. Getz, RNA sequence analysis reveals macroscopic somatic clonal expansion across normal tissues, *Science* (2019) 364.
- [19] M. DuPage, A.L. Dooley, T. Jacks, Conditional mouse lung cancer models using adenoviral or lentiviral delivery of Cre recombinase, *Nat. Protoc.* 4 (2009) 1064–1072.
- [20] M.C. Kwon, A. Berns, Mouse models for lung cancer, *Mol. Oncol.* 7 (2013) 165–177.
- [21] Y. Li, Z. Lv, S. Zhang, Z. Wang, L. He, M. Tang, W. Pu, H. Zhao, Z. Zhang, Q. Shi, D. Cai, M. Wu, G. Hu, K.O. Lui, J. Feng, M.A. Nieto, B. Zhou, Genetic fate mapping of transient cell fate reveals N-cadherin activity and function in tumor metastasis, *Dev. Cell* 54 (2020) 593–607 e595.
- [22] Y. Takeuchi, T. Tanegashima, E. Sato, T. Irie, A. Sai, K. Itahashi, S. Kumagai, Y. Tada, Y. Togashi, S. Koyama, E.A. Akbay, T. Karasaki, K. Kataoka, S. Funaki, Y. Shintani, I. Nagatomo, H. Kida, G. Ishii, T. Miyoshi, K. Aokage, K. Kakimi, S. Ogawa, M. Okumura, M. Eto, A. Kumanogoh, M. Tsuibo, H. Nishikawa, Highly immunogenic cancer cells require activation of the WNT pathway for immunological escape, *Sci Immunol* 6 (2021), eabc6424.
- [23] D.J. Stewart, Wnt signaling pathway in non-small cell lung cancer, *J. Natl. Cancer Inst.* 106 (2014) djt356.
- [24] N. Vasan, J. Baselga, D.M. Hyman, A view on drug resistance in cancer, *Nature* 575 (2019) 299–309.
- [25] D.R. Green, The coming decade of cell death research: five riddles, *Cell* 177 (2019) 1094–1107.
- [26] W. Min, C. He, S. Zhang, Y. Zhao, c-Src increases the sensitivity to TKIs in the EGFR-mutant lung adenocarcinoma, *Front. Oncol.* 11 (2021), 602900.
- [27] K. Liu, L. Gao, X. Ma, J.J. Huang, J. Chen, L. Zeng, C.R. Ashby Jr., C. Zou, Z. S. Chen, Long non-coding RNAs regulate drug resistance in cancer, *Mol. Cancer* 19 (2020) 54.
- [28] W.L. Hu, L. Jin, A. Xu, Y.F. Wang, R.F. Thorne, X.D. Zhang, M. Wu, GUARDIN is a p53-responsive long non-coding RNA that is essential for genomic stability, *Nat. Cell Biol.* 20 (2018) 492–502.
- [29] L.M. Cumbo Garcia, T.E. Peterson, M.A. Cepeda, A.J. Johnson, L.F. Parney, Isolation and analysis of plasma-derived exosomes in patients with glioma, *Front. Oncol.* 9 (2019) 651.
- [30] M.S. Brown, B. Abdollahi, O.M. Wilkins, H. Lu, P. Chakraborty, N.B. Ognjenovic, K. E. Muller, M.K. Jolly, B.C. Christensen, S. Hassanpour, D.R. Pattabiraman, Phenotypic heterogeneity driven by plasticity of the intermediate EMT state governs disease progression and metastasis in breast cancer, *Sci. Adv.* 8 (2022), eabj8002.
- [31] S. Brabletz, H. Schuhwerk, T. Brabletz, M.P. Stemmler, Dynamic EMT: a multi-tool for tumor progression, *EMBO J.* 40 (2021), e108647.
- [32] I. Pastushenko, F. Mauri, Y. Song, F. de Cock, B. Meeusen, B. Swedlund, F. Impens, D. Van Haver, M. Opitz, M. Thery, Y. Bareche, G. Lapouge, M. Vermeersch, Y. R. Van Eycke, C. Balsat, C. Decaestecker, Y. Sokolow, S. Hassid, A. Perez-Bustillo, B. Agreda-Moreno, L. Rios-Buceta, P. Jaen, P. Redondo, R. Sieira-Gil, J.F. Millan-Cayetano, O. Sanmatrin, N. D'Haene, V. Moers, M. Rozzi, J. Blondeau, S. Lemaire, S. Sczzaro, V. Janssens, M. De Troya, C. Dubois, D. Perez-Morga, I. Salmon, C. Sotiriou, F. Helmbacher, C. Blanpain, Fat1 deletion promotes hybrid EMT state, tumour stemness and metastasis, *Nature* 589 (2021) 448–455.
- [33] C. Kroger, A. Afeyan, J. Mraz, E.N. Eaton, F. Reinhardt, Y.L. Khodor, P. Thiru, B. Bierie, X. Ye, C.B. Burge, R.A. Weinberg, Acquisition of a hybrid E/M state is essential for tumorigenicity of basal breast cancer cells, *Proc. Natl. Acad. Sci. U. S. A.* 116 (2019) 7353–7362.
- [34] J. Dong, Y. Hu, X. Fan, X. Wu, Y. Mao, B. Hu, H. Guo, L. Wen, F. Tang, Single-cell RNA-seq analysis unveils a prevalent epithelial/mesenchymal hybrid state during mouse organogenesis, *Genome Biol.* 19 (2018) 31.
- [35] A.M. Richardson, L.S. Havel, A.E. Koyen, J.M. Konen, J. Shupe, W.G.t. Wiles, W. D. Martin, H.E. Grossniklaus, G. Sica, M. Gilbert-Ross, A.I. Marcus, Vimentin is required for lung adenocarcinoma metastasis via heterotypic tumor cell-cancer-associated fibroblast interactions during collective invasion, *Clin. Cancer Res.* 24 (2018) 420–432.
- [36] S.C. Johnson, S.E. McClelland, Watching cancer cells evolve through chromosomal instability, *Nature* 570 (2019) 166–167.
- [37] E.C. d'Bruin, N. McGranahan, R. Mitter, M. Salm, D.C. Wedge, L. Yates, M. Jamal-Hanjani, S. Shafi, N. Murugesa, A.J. Rowan, E. Gronroos, M.A. Muhammad, S. Horswell, M. Gerlinger, I. Varela, D. Jones, J. Marshall, T. Voet, P. Van Loo, D. M. Rassl, R.C. Rintoul, S.M. Janes, S.M. Lee, M. Forster, T. Ahmad, D. Lawrence, M. Falzon, A. Capitanio, T.T. Harkins, C.C. Lee, W. Tom, E. Teeff, S.C. Chen, S. Begum, A. Rabinowitz, B. Phillipore, B. Spencer-Dene, G. Stamp, Z. Szallasi, N. Matthews, A. Stewart, P. Campbell, C. Swanton, Spatial and temporal diversity in genomic instability processes defines lung cancer evolution, *Science* 346 (2014) 251–256.
- [38] Z. Chen, C.M. Fillmore, P.S. Hammerman, C.F. Kim, K.K. Wong, Non-small-cell lung cancers: a heterogeneous set of diseases, *Nat. Rev. Cancer* 14 (2014) 535–546.
- [39] M. Sorin, M. Rezanejad, E. Karimi, B. Fiset, L. Desharnais, L.J.M. Perus, S. Milette, M.W. Yu, S.M. Maritan, S. Dore, E. Pichette, W. Enlow, A. Gagne, Y. Wei, M. Orain, V.S.K. Manem, R. Rayes, P.M. Siegel, S. Camilleri-Broet, P.O. Fiset, P. Desmeules, J. D. Spicer, D.F. Quail, P. Joubert, L.A. Walsh, Single-cell spatial landscapes of the lung tumour immune microenvironment, *Nature* 614 (2023) 548–554.
- [40] A.M. Leader, J.A. Grout, B.B. Maier, B.Y. Nabet, M.D. Park, A. Tabachnikova, C. Chang, L. Walker, A. Lansky, J. Le Beriche, L. Troncoso, N. Malissen, D. Davila, J.C. Martin, G. Magri, K. Tuballes, Z. Zhao, F. Petralia, R. Samstein, N.R. D'Amore, G. Thurston, A.O. Kamphorst, A. Wolf, R. Flores, P. Wang, S. Muller, I. Mellman, M. B. Beasley, H. Salmon, A.H. Rahman, T.U. Marron, E. Kenigsberg, M. Merad, Single-cell analysis of human non-small cell lung cancer lesions refines tumor classification and patient stratification, *Cancer Cell* 39 (2021) 1594–1609 e1512.
- [41] C. Wang, J. Dai, N. Qin, J. Fan, H. Ma, C. Chen, M. An, J. Zhang, C. Yan, Y. Gu, Y. Xie, Y. He, Y. Jiang, M. Zhu, C. Song, T. Jiang, J. Liu, J. Zhou, N. Wang, T. Hua, S. Liang, L. Wang, J. Xu, R. Yin, L. Chen, L. Xu, G. Jin, D. Lin, Z. Hu, H. Shen, Analyses of Rare Predisposing Variants of Lung Cancer in 6,004 Whole Genomes in Chinese, *Cancer Cell*, 2022.
- [42] N.D. Marjanovic, M. Hofree, J.E. Chan, D. Canner, K. Wu, M. Trakala, G. G. Hartmann, O.C. Smith, J.Y. Kim, K.V. Evans, A. Hudson, O. Ashenberg, C.B. M. Porter, A. Bejnood, A. Subramanian, K. Pittier, Y. Yan, T. Delorey, D.R. Phillips, N. Shah, O. Chaudhary, A. Tsankov, T. Hollmann, N. Rekhtman, P.P. Mission, J. T. Poirier, L. Mazutis, R. Li, J.H. Lee, A. Amon, C.M. Rudin, T. Jacks, A. Regev,

- T. Tammela, Emergence of a high-plasticity cell state during lung cancer evolution, *Cancer Cell* 38 (2020) 229–246 e213.
- [43] Q. Hu, H. Ma, H. Chen, Z. Zhang, Q. Xue, LncRNA in tumorigenesis of non-small-cell lung cancer: from bench to bedside, *Cell Death Dis.* 8 (2022) 359.
- [44] C. Swanton, Take lessons from cancer evolution to the clinic, *Nature* 581 (2020) 382–383.
- [45] D. Leveque, Pharmacokinetic interactions of dasatinib and docetaxel, *Lancet Oncol.* 15 (2014) e51.
- [46] J. Li, U. Rix, B. Fang, Y. Bai, A. Edwards, J. Colinge, K.L. Bennett, J. Gao, L. Song, S. Eschrich, G. Superti-Furga, J. Koomen, E.B. Haura, A chemical and phosphoproteomic characterization of dasatinib action in lung cancer, *Nat. Chem. Biol.* 6 (2010) 291–299.
- [47] E. Gordian, J. Li, Y. Pevzner, M. Mediavilla-Varela, K. Luddy, K. Ohaegbulam, K. G. Daniel, E.B. Haura, T. Munoz-Antonia, Transforming growth factor beta signaling overcomes dasatinib resistance in lung cancer, *PLoS One* 9 (2014), e114131.
- [48] K.A. Gold, J.J. Lee, N. Harun, X. Tang, J. Price, J.D. Kawedia, H.T. Tran, J. J. Erasmus, G.R. Blumenschein, W.N. William, Wistuba II, F.M. Johnson, A phase I/II study combining erlotinib and dasatinib for non-small cell lung cancer, *Oncol.* 19 (2014) 1040–1041.
- [49] E.M. Beauchamp, B.A. Woods, A.M. Dulak, L. Tan, C. Xu, N.S. Gray, A.J. Bass, K. K. Wong, M. Meyerson, P.S. Hammerman, Acquired resistance to dasatinib in lung cancer cell lines conferred by DDR2 gatekeeper mutation and NF1 loss, *Mol. Cancer Therapeut.* 13 (2014) 475–482.